Synthesis of diphosphine-substituted selenido carbonyl iron clusters: progressive deformation of the Fe_3Se_2 core in the *nido* clusters $[Fe_3Se_2(CO)_7\{\mu\text{-}(Ph_2P)_2R\}]$ by widening the bite of the bridging ligand [1]

Daniele Cauzzi, Claudia Graiff, Maurizio Lanfranchi, Giovanni Predieri, Antonio Tiripicchio *

Dipartimento di Chimica Generale ed Inorganica, Chimica Analitica, Chimica Fisica, Università di Parma, Centro di Studio per la Strutturistica Diffrattometrica del CNR, Viale delle Scienze, I-43100 Parma, Italy

Abstract

The reactions of $[Fe_3(CO)_{12}]$ with three diphosphine diselenides, $dppmSe_2$, $dppeSe_2$ and $dppfcSe_2$, produce the disubstituted clusters $[Fe_3(\mu_3\text{-}Se)_2(CO)_7\{(Ph_2P)_2R\}]$ ($R = CH_2$ (dppm) **3**; $R = CH_2CH_2$ (dppe) **7**; $R = (C_5H_4)_2Fe$ (dppfc) **8**) as the main products. Other products are $[Fe_3(\mu_3Se)_2(CO)_9]$ **1**, $[Fe(CO)_4(dppm)]$ **2**, $[Fe_2(\mu\text{-}Se_2)(CO)_4(dppm)]$ **4** in the case of dppm and $[\{Fe_3(\mu_3\text{-}Se)_2(CO)_8\}_2(dppe)]$ **5** in the case of dppe. Clusters **1**, **3**, **5**, **7** and **8** have a square-pyramidal structure with two iron and two selenium atoms alternating in the basal plane and the third iron atom (Fe_{ap}) at the apex of the pyramid, and should be regarded as *nido*-clusters with seven skeletal electron pairs. The phosphine substitution is regioselective, occurring only on the two basal iron atoms. ^1H and ^{31}P NMR data in solution suggest a fluxional behaviour for **3** and **7** in solution due to the migration of a metal–metal bond to link the two iron atoms bound to the bidentate ligand. This is probably related to the deformation of the Fe_3Se_2 core induced by the steric demand of the diphosphines in such a way that the $Fe \cdots Fe$ non-bonding distance decreases as the bite of the ligand shortens. The crystal structures of **3**, **4**, **5**, **7** and **8** are described. © 1997 Elsevier Science S.A.

Keywords: Iron; Selenium; Carbonyl; Clusters; Crystal structures

1. Introduction

Tertiary phosphine chalcogenides R_3PE ($E = S$, Se or Te) have served as useful starting compounds for the synthesis of transition metal clusters containing bridging chalcogenido ligands by reaction with metal carbonyl complexes [1–6]. This simple synthetic procedure takes advantage of the frailty of the $P=E$ bond, which makes easy the formation of phosphine-substituted chalcogenide clusters through oxidative transfer of chalcogen atoms to low-valent metal species.

Previously [4,5], we reported the reactions of Ph_3PSe with $[Fe_3(CO)_{12}]$ and $[Ru_3(CO)_{12}]$. In the case of iron the reaction afforded several dinuclear and trinuclear
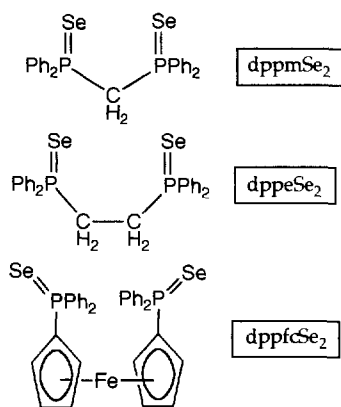
compounds, whereas in the case of ruthenium the same reaction was found to be quite selective, giving the disubstituted trinuclear cluster $[Ru_3(\mu_3\text{-}Se)_2(CO)_7(PPh_3)_2]$ in very high yield, with minor amounts of other products.

Furthermore, we found [6] that the diphosphine diselenide $(Ph_2PSe)_2CH_2$ ($dppmSe_2$) and $[Ru_3(CO)_{12}]$ react in toluene to give $[Ru_3(\mu_3\text{-}Se)_2(CO)_7(dppm)]$, $[Ru_4(\mu_4\text{-}Se)_2(CO)_9(dppm)]$ and $[Ru_4(\mu_3\text{-}Se)_4(CO)_{10}(dppm)]$ ($dppm = (Ph_2P)_2CH_2$), which is the first reported 72-electron Ru–Se cubane-like cage complex.

With the aim of producing a workable amount of diphosphine substituted $Fe_xSe_y(CO)_z$ derivatives as useful starting materials for cluster-growth reactions, we have reacted $[Fe_3(CO)_{12}]$ with three diphosphine diselenides of general formula $(Ph_2PSe)_2R$, differing for the nature of the bridging group R: $R = CH_2$, $dppmSe_2$; $R = CH_2CH_2$, $dppeSe_2$; $R = (C_5H_4)_2Fe$, $dppfcSe_2$ (Scheme 1). The present paper deals with these reac-

---

* Corresponding author.
[1] Dedicated to the memory of Professor Yuri Struchkov in recognition of his important contributions to structural organometallic chemistry.

Scheme 1.

tions and with the description of the structural features of five iron-selenido clusters.

2. Experimental

2.1. Materials and analytical equipment

The starting reagents $Fe_3(CO)_{12}$, KSeCN, Se and the diphosphines $(Ph_2P)_2R$ ($R = CH_2$ (dppm); $R = CH_2CH_2$ (dppe); $R = (C_5H_4)_2Fe$ (dppfc)) were pure commercial products (Aldrich and Fluka), and were used as received. The solvents (Carlo Erba) were dried and distilled by standard techniques before use. All manipulation (prior to the TLC separations) were carried out under dry nitrogen by means of standard Schlenk-tube techniques.

Elemental (C, H) analyses were performed with a Carlo Erba EA 1108 automated analyzer. IR spectra (KBr discs or CH_2Cl_2 solutions) were recorded on a Nicolet 5PC FT spectrometer. ^1H, ^{31}P (81.0 MHz; 85% H_3PO_4 as external reference) and ^{77}Se (38.2 MHz; Ph_2Se_2 in $CHCl_3$ [+461 ppm relative to Me_2Se] as external reference) NMR spectra were recorded for $CHCl_3$-d_1 solutions on Bruker instruments AC300 (^1H) and CXP 200 (^{31}P and ^{77}Se).

2.2. Preparation and reactions

2.2.1. Preparation of the diphosphine diselenides

The ligands $dppmSe_2$ [7] and $dppeSe_2$ [8] were prepared according to literature methods by selenium transfer from elemental Se and KSeCN respectively. DppfcSe_2 is a new compound; it was prepared by a slight modification of the method described for dppe: a solution of KSeCN (0.5 g) and dppfc (0.1 g) in acetonitrile (100 ml) was stirred for 6 h at room temperature; the solvent was removed in vacuo and the residue extracted with water. The rough powder was recrystallized from toluene, obtaining a brownish yellow product. Yield

80%. Anal. Found: C, 57.4; H, 4.4. $C_{34}H_{28}FeP_2Se_2$ Calc.: C, 57.3; H, 4.0%. FTIR (KBr) (cm^{-1}): 533 vs (νPSe). ^1H NMR ($CHCl_3$-d_1): δ 7.26–7.65 (m, 20H, Ph), 4.31 (t, 4H, fc), 4.69 (t, 4H, fc). ^{31}P NMR ($CHCl_3$-d_1): δ 31.5 (s, with ^{77}Se satellites: ^1J(P,Se) 737 Hz).

2.2.2. Reaction of $[Fe_3(CO)_{12}]$ with $dppmSe_2$

Treatment of $[Fe_3(CO)_{12}]$ (150 mg, 0.3 mmol) with 161 mg of $dppmSe_2$ (0.3 mmol) for 3 h in hot toluene (70 °C) under N_2 gave a deep brown solution which, upon TLC purification, yielded violet $[Fe_3(\mu_3$-$Se)_2(CO)_9]$ 1 (48%), yellow $[Fe(CO)_4(dppm)]$ 2 (8.7%), black $[Fe_3(\mu_3$-$Se)_2(CO)_7(dppm)]$ 3 (22%), orange $[Fe_2(\mu$-$Se_2)(CO)_4(dppm)]$ 4 (10%) and some decomposition. Careful crystallization of a sample of clusters 3 and 4 (from a CH_2Cl_2/MeOH mixture at 5 °C for some days) gave well-formed crystals suitable for X-ray analysis; compounds 1 and 2 were identified by comparison of their spectroscopic data with those reported in the literature. Complex 1. IR (CH_2Cl_2, νCO, cm^{-1}): 2056 vs, 2036 s, 2013 s, 1972 sh. Complex 2. IR (CH_2Cl_2, νCO, cm^{-1}): 2056 vs, 2006 w, 1972 w, 1938 s. ^1H NMR ($CHCl_3$-d_1): δ 3.31 (d, 2H, CH_2, J(H,P) 9 Hz). ^{31}P NMR ($CHCl_3$-d_1): δ 65.7 (d, J(P,P) 74 Hz), −25.05 (d, J(P,P) 74 Hz). Complex 3. IR (CH_2Cl_2, νCO, cm^{-1}): 2052 s, 2040 s, 1993 vs, 1942 w. ^1H NMR ($CHCl_3$-d_1): δ 4.08 (t, 2H, CH_2, J(H,P) 10.5 Hz), 3.22 (t, 2H, CH_2, J(H,P) 10.5 Hz). ^{31}P NMR ($CHCl_3$-d_1): δ 77.7 (s), 53.0 (d, J(P,P) 58 Hz), 42.6 (d, J(P,P) 58 Hz). ^{77}Se NMR ($CHCl_3$-d_1): 248.7 (t, J(Se,P) 14 Hz). Complex 4. IR (CH_2Cl_2, νCO, cm^{-1}): 2055 s, 1990 s, 1956 vs, 1923 s. ^1H NMR ($CHCl_3$-d_1): δ 4 (m br, 2H, CH_2). ^{31}P NMR ($CHCl_3$-d_1): δ 63.4 (s).

2.2.3. Reaction of $[Fe_3(CO)_{12}]$ with $dppeSe_2$

Treatment of $[Fe_3(CO)_{12}]$ (181 mg, 0.36 mmol) with 200 mg of $dppeSe_2$ (0.36 mmol) for 3 h in hot toluene (70 °C) under N_2 gave a deep brown solution which, upon TLC purification, yielded violet $[Fe_3(\mu_3$-$Se)_2(CO)_9]$ 1 (34%), violet $[\{Fe_3(\mu_3$-$Se)_2(CO)_8\}_2(dppe)]$ 5 (23%), a small amount of a violet compound 6, a probable isomer of $[\{Fe_3(\mu_3$-$Se)_2(CO)_8\}_2(dppe)]$, brown $[Fe_3(\mu_3$-$Se)_2(CO)_7(dppe)]$ 7 (30%) and some decomposition. Careful crystallization of a sample of clusters 5 and 7 (from a CH_2Cl_2/MeOH mixture at 5 °C for some days) gave well-formed crystals suitable for X-ray analysis; isomer 6 was identified by comparison of its spectroscopic data with those of compound 5. Complex 5. IR (CH_2Cl_2, νCO, cm^{-1}): 2066 s, 2027 vs, 2003 vs, 1940 w. ^1H NMR ($CHCl_3$-d_1): δ 3.71 (m br, 2H, CH_2). ^{31}P NMR ($CHCl_3$-d_1): δ 61.9 (s br). Complex 6. IR (CH_2Cl_2, νCO, cm^{-1}): 2067 s, 2025 vs, 1998 vs, 1948 w, 1969 w. ^{31}P NMR ($CHCl_3$-d_1): δ 61.3 (s br). Complex 7. IR (CH_2Cl_2, νCO, cm^{-1}): 2052 vs, 2040 w, 2011 s, 1986 s, 1951 sh. ^1H NMR ($CHCl_3$-d_1): δ

2.71 (m br, 2H, CH_2), 2.41 (m br, 2H, CH_2). ^{31}P NMR ($CHCl_3$-d_1): δ 75.9 (s), 71 (s br), 68.3 (s), 48.1 (s).

2.2.4. Reaction of [Fe₃(CO)₁₂] with dppfcSe₂

Treatment of [$Fe_3(CO)_{12}$] (148 mg, 0.29 mmol) with 210 mg of dppfcSe₂ (0.29 mmol) for 3 h in hot toluene (70 °C) under N_2 gave a deep brown solution which, upon TLC purification, yielded black [$Fe_3(\mu_3$-Se)$_2$(CO)$_7$(dppfc)] **8** (16%), a small amount of [{$Fe_3(\mu_3$-Se)$_2$(CO)$_5$}$_2$(dppfc)] **9** and some decomposition. Careful crystallization of a sample of cluster **8** (from a CH_2Cl_2/MeOH mixture at 5 °C for some days) gave well-formed crystals suitable for X-ray analysis; compound **9** was identified by comparison of its spectroscopic data with those of compounds **5** and **6**. Complex **8**. IR (CH_2Cl_2, νCO, cm^{-1}): 2055 w, 2039 vs, 2001 s, 1980 w, 1941 w. ^{31}P NMR ($CHCl_3$-d_1): δ 73.7 (s). Complex **9**. IR (CH_2Cl_2, νCO, cm^{-1}): 2065 s, 2026 vs, 2002 vs, 1941 w. ^{31}P NMR ($CHCl_3$-d_1): δ 66.3 (s).

2.3. X-ray data collection, structure solution and refinement for [Fe₃(μ₃-Se)₂(CO)₇(dppm)] 3, [Fe₂(μ-Se₂)(CO)₄(dppm)] 4, [{Fe₃(μ₃-Se)₂(CO)₂}₂(dppe)} 5, [Fe₃(μ₃-Se)₂(CO)₇(dppe)] 7 and [Fe₃(μ₃-Se)₂(CO)₇(dppfc)] · CHCl₃ 8 · CHCl₃

The crystallographic data for compounds **3**, **4**, **5**, **7** and **8** · CHCl₃ are summarized in Table 1. Accurate unit cell parameters were obtained by using the setting angles of 30 high-angle reflections; no significant decay was noticed over the time of data collection for all compounds. Intensities were corrected for Lorentz and polarization effects. A correction for absorption was applied for **5** [maximum and minimum value for the transmission coefficient 1.0000 and 0.5909] [9].

All five structures were solved by Patterson methods of SHELXS-86 [10] and refined by full-matrix least-squares (blocked full-matrix for **4**, **5** and **8** · CHCl₃), using the SHELX-76 program [11], first with isotropic thermal parameters and then with anisotropic thermal

Table 1
Summary of crystallographic data for the complexes **3, 4, 5, 7, 8**

	3	4	5	7	8
Formula	$C_{32}H_{22}Fe_3$ $O_7P_2Se_2$	$C_{29}H_{22}Fe_2$ $O_4P_2Se_2$	$C_{42}H_{24}Fe_6$ $O_{16}P_2Se_4$	$C_{33}H_{24}Fe_3$ $O_7P_2Se_2$	$C_{41}H_{28}Fe_4$ $O_7P_2Se_2 \cdot CHCl_3$
Molecular weight	905.93	766.05	1497.51	919.96	1195.30
Crystal system	triclinic	triclinic	monoclinic	monoclinic	monoclinic
Space group	$P\bar{1}$	$P\bar{1}$	$P2_1/n$	$P2_1/c$	$P2_1/n$
Radiation λ (Å)	graphite monochromated	Nb-filtered	graphite monochromated	graphite monochromated	Nb-filtered
Mo K α (0.71073 Å)					
a (Å)	11.059(5)	10.418(2)	9.241(4)	13.353(5)	16.986(5)
b (Å)	11.678(5)	15.888(3)	13.891(5)	10.788(4)	12.334(4)
c (Å)	14.507(6)	17.983(4)	19.708(6)	24.812(6)	23.062(6)
α (°)	100.74(2)	86.89(1)			
β (°)	95.80(2)	89.39(1)	94.98(2)	102.15(2)	110.16(2)
γ (°)	112.16(2)	78.79(1)			
V (Å³)	1674(1)	2915(1)	2520(2)	3494(2)	4536(2)
Z	2	4	2	4	4
D_{calc} (g cm⁻³)	1.797	1.745	1.793	1.749	1.750
F(000)	892	1512	1452	1816	2360
Crystal size (mm³)	0.18 × 0.32 × 0.38	0.15 × 0.28 × 0.31	0.10 × 0.21 × 0.25	0.13 × 0.23 × 0.34	0.23 × 0.27 × 0.38
μ(Mo K α) (cm⁻¹)	35.98	36.35	46.99	34.49	31.54
Diffractometer	Philips PW 1100	Siemens AED	Philips PW 1100	Philips PW 1100	Philips PW 1100
Scan type	$\theta/2\theta$	$\theta/2\theta$	$\theta/2\theta$	$\theta/2\theta$	$\theta/2\theta$
Scan speed (° min⁻¹)	3-10	3-12	3-10	2-10	3-12
θ range (°)	3-27	3-27	3-30	3-25	3-25
Standard reflections every 100	one measured every 100	one measured every 100	one measured every 100	one measured every 100	one measured every 100
Reflections measured	±n, ±k, l	h, ±k, l	±h, k, l	±h, k, l	±h, k, l
Unique total data	7301	12723	5501	6156	7973
Unique observed data	3006 [$I > 2\sigma(I)$]	6905 [$I > 3\sigma(I)$]	2992 [$I > 2\sigma(I)$]	1118 [$I > 2\sigma(I)$]	4210 [$I > 2\sigma(I)$]
ᵃ R	0.0485	0.0679	0.0354	0.0326	0.0486
ᵇ R_w	0.0607	0.0718	0.0379	0.0410	0.0554

ᵃ $R = \Sigma ||F_o| - |F_c||/\Sigma|F_o|$.
ᵇ $R_w = [\Sigma w(|F_o| - |F_c|)^2/\Sigma w(F_o)^2]$.

parameters for all non-hydrogen atoms for **4** and **5**, except for the carbon atoms of the phenyl rings and solvent molecules when present, for **3** and **8** · $CHCl_3$ and only for Se, Fe, P atoms for **7**. The $CHCl_3$ molecule of solvation in **8** · $CHCl_3$ was found disordered, with the carbon atom distributed in two equivalent positions and the three chlorine atoms in three positions with occupancy factors 0.5, 0.25 and 0.25 respectively. The hydrogen atoms were placed at their geometrically cal-

Table 2
Atomic coordinates ($\times 10^4$) and isotropic thermal parameters ($\text{Å}^2 \times 10^4$) for the non-hydrogen atoms of the complex **3**

Atom	x	y	z	U
Se(1)	-838.7(9)	2703.5(9)	2605.7(6)	311(4) [a]
Se(2)	290.1(9)	1501.6(8)	962.5(6)	290(4) [a]
Fe(1)	453.6(12)	3606.2(11)	1519.9(8)	262(5) [a]
Fe(2)	-1848.1(12)	1517.8(13)	1012.9(9)	340(6) [a]
Fe(3)	-549.5(12)	783.4(12)	2283.2(9)	291(5) [a]
P(1)	2325(2)	4245(2)	2533(2)	245(9) [a]
P(2)	1380(2)	1696(2)	3306(2)	258(9) [a]
O(1)	156(9)	6012(7)	1986(6)	691(45) [a]
O(2)	1672(7)	4349(7)	-106(5)	551(35) [a]
O(3)	-4310(9)	1555(13)	1545(8)	1249(73) [a]
O(4)	-2010(9)	2760(8)	-555(6)	820(45) [a]
O(5)	-3090(8)	-1139(8)	-81(7)	936(49) [a]
O(6)	-500(9)	-1701(7)	1536(6)	710(43) [a]
O(7)	-2616(8)	-376(8)	3337(6)	750(42) [a]
C(1)	232(9)	5058(10)	1807(6)	387(45) [a]
C(2)	1186(9)	4056(9)	524(7)	348(41) [a]
C(3)	-3337(12)	1539(14)	1363(9)	725(68) [a]
C(4)	-1885(11)	2346(10)	93(8)	525(54) [a]
C(5)	-2584(10)	-97(10)	351(9)	522(53) [a]
C(6)	-533(10)	-730(10)	1832(7)	410(45) [a]
C(7)	-1766(9)	89(9)	2951(7)	393(42) [a]
C(8)	2674(8)	2947(8)	2906(6)	265(36) [a]
C(9)	2635(8)	5411(8)	3676(6)	279(20)
C(10)	1578(10)	5541(9)	4063(7)	398(24)
C(11)	1854(10)	6346(9)	4975(7)	471(27)
C(12)	3100(10)	6996(10)	5485(8)	538(29)
C(13)	4132(11)	6898(10)	5094(8)	515(29)
C(14)	3916(9)	6p89(9)	4186(7)	398(24)
C(15)	3792(8)	5024(8)	2037(6)	285(20)
C(16)	4583(8)	4440(8)	1695(6)	347(22)
C(17)	5659(10)	5082(10)	1287(7)	515(28)
C(18)	5913(10)	6285(10)	1192(8)	546(30)
C(19)	5090(10)	6861(11)	1509(8)	568(29)
C(20)	4030(9)	6251(9)	1924(7)	447(26)
C(21)	1449(8)	2417(8)	4555(6)	264(20)
C(22)	2562(10)	3405(10)	5115(7)	476(27)
C(23)	2618(10)	3859(10)	6079(7)	487(27)
C(24)	1584(10)	3302(10)	6505(8)	543(29)
C(25)	447(11)	2310(11)	5966(8)	605(31)
C(26)	372(10)	1863(10)	4991(7)	451(26)
C(27)	2284(8)	686(8)	3438(6)	303(21)
C(28)	2597(9)	428(9)	4302(7)	426(25)
C(29)	3306(10)	-336(10)	4371(8)	540(29)
C(30)	3718(11)	-824(11)	3599(8)	608(31)
C(31)	3386(11)	-587(11)	2727(9)	682(34)
C(32)	2689(10)	172(10)	2641(8)	534(29)

[a] U_{eq} defined as one-third of the trace of the orthogonalized $\mathbf{U}_{ij}$ tensor.

culated positions (C–H = 0.96 Å) and refined 'riding' on the corresponding carbon atoms, except for those of the CH_2 group of **5** and those of the Cp rings of **8** · $CHCl_3$ that were clearly found and refined isotropically. The final cycles of refinement were carried out on the basis of 296 variables for **3**, 707 for **4**, 323 for **5**, 227 for **7** and 465 for **8** · $CHCl_3$. The biggest remaining peak (close to one heavy atom) in the final difference map was equivalent to about 1.37 for **3**, 1.92 for **4**, 0.61 for **5**, 0.43 for **7** and 0.71 e Å^{-3} for **8** · $CHCl_3$. A weighting scheme $w = K[\sigma^2(F_o) + gF_o^2]^{-1}$ was used in the last cycles of refinement with $K = 1.0000$ and $g = 0.0037$ (**3**), $K = 0.3830$ and $g = 0.0026$ (**7**), $K = 0.9008$ and $g = 0.0012$ (**8** · $CHCl_3$) at convergence, unit weight was used for **4** and **5**. Atomic scattering factors and anomalous scattering coefficients were taken from Ref. [12]. All calculations were carried out on the Gould Powernode 6040 and Encore 91 computers of the Centro di Studio per la Strutturistica Diffrattometrica, CNR, Parma.

Atomic coordinates for the non-hydrogen atoms are given in Table 2, Table 3, Table 4, Tables 5 and 6. Hydrogen atom coordinates, anisotropic thermal parameters and complete lists of bond lengths and angles have been deposited at the Cambridge Crystallographic Data Centre.

3. Results and discussion

3.1. Reactions of [Fe₃(CO)₁₂] with the diphosphine diselenides dppmSe₂, dppeSe₂ and dppfcSe₂ and spectroscopic characterizations

The reactions of $[Fe_3(CO)_{12}]$ with three diphosphine diselenides dppmSe$_2$, dppeSe$_2$ and dppfcSe$_2$ produce the disubstituted clusters $[Fe_3(\mu_3\text{-Se})_2(CO)_7\{(Ph_2P)_2R\}]$ (R = CH$_2$ **3**; R = CH$_2$CH$_2$ **7**; R = (C$_5$H$_4$)$_2$Fe **8**) as the main products. In particular, the reactions with dppeSe$_2$ and dppfcSe$_2$ afford **7** and **8** along with other complexes, which contain the same cluster core Fe$_3$Se$_2$; these are the unsubstituted cluster **1** and the double monosubstituted derivatives **5**, **6** and **9**, where dppe and dppfc bridge two cluster units. On the contrary, the reaction with dppmSe$_2$ gives rise also to lower nuclearity products, namely to the mononuclear $[Fe(CO)_4(dppm)]$ **2** and to the dinuclear derivative $[Fe_2(\mu\text{-Se}_2)(CO)_4(dppm)]$ **4**.

Compounds **3**, **4**, **5**, **7** and **8** were unequivocally identified by solving their crystal structures, whereas compounds **1** [13] and **2** [14] were identified by comparison with the spectral data reported in the literature. The structures of compounds **6** and **9** (two cluster units linked by dppe or dppfc respectively) were deduced by comparison of their spectral data with those of **5**. In

Table 3

Atomic coordinates ($\times 10^4$) and equivalent isotropic thermal parameters ($\mathring{A}^2 \times 10^4$) defined as one-third of the trace of the orthogonalized U_{ij} tensor, for the non-hydrogen atoms of the complex **4**

Atom	x	y	z	U_{eq}
Se(1A)	5295.5(12)	-852.1(7)	8491.0(7)	539(4)
Se(2A)	3070.4(11)	-689.3(6)	8367.6(7)	471(4)
Fe(1A)	4156.0(14)	-1682.0(8)	9310.8(9)	390(5)
Fe(2A)	4433.2(14)	-1916.8(9)	7905.9(9)	404(5)
P(1A)	2798(3)	-2564(2)	9523(2)	360(8)
P(2A)	2868(3)	-2648(2)	7841(2)	369(8)
O(1A)	3494(10)	-638(6)	10589(5)	780(39)
O(2A)	6275(9)	-3004(5)	9918(6)	785(38)
O(3A)	6535(9)	-3398(5)	8184(6)	748(37)
O(4A)	4834(11)	-1591(6)	6320(6)	851(44)
C(1A)	3754(12)	-1048(7)	10088(7)	550(43)
C(2A)	5445(11)	-2477(8)	9678(7)	558(43)
C(3A)	5702(11)	-2819(8)	8066(7)	539(42)
C(4A)	4647(11)	-1706(6)	6951(7)	520(42)
C(5A)	2711(10)	-3244(5)	8734(6)	382(32)
C(6A)	3277(10)	-3347(6)	10308(6)	421(34)
C(7A)	3486(12)	-4238(6)	10237(6)	545(42)
C(8A)	3842(14)	-4785(8)	10863(7)	681(51)
C(9A)	4009(14)	-4483(9)	11535(8)	788(59)
C(10A)	3785(15)	-3598(9)	11607(7)	739(57)
C(11A)	3402(14)	-3049(8)	10978(7)	710(53)
C(12A)	1099(10)	-2141(6)	9738(6)	453(36)
C(13A)	291(11)	-2679(7)	10034(7)	543(42)
C(14A)	-1029(13)	-2377(9)	10165(9)	758(58)
C(15A)	-1567(12)	-1505(8)	10005(8)	721(53)
C(16A)	-755(11)	-970(8)	9741(8)	613(46)
C(17A)	541(11)	-1261(6)	9614(7)	523(41)
C(18A)	3040(11)	-3498(6)	7181(6)	430(35)
C(19A)	4220(12)	-3765(7)	6823(7)	579(45)
C(20A)	4335(14)	-4411(8)	6298(8)	701(52)
C(21A)	3299(14)	-4786(8)	6174(8)	691(54)
C(22A)	2130(15)	-4533(8)	6526(8)	719(56)
C(23A)	2002(13)	-3896(7)	7039(7)	607(47)
C(24A)	1204(10)	-2043(6)	7648(6)	425(35)
C(25A)	108(11)	-2188(8)	7975(8)	639(48)
C(26A)	-1126(12)	-1732(9)	7790(7)	638(49)
C(27A)	-1224(15)	-1115(10)	7206(10)	837(65)
C(28A)	-156(15)	-955(9)	6858(9)	770(58)
C(29A)	1077(13)	-1415(7)	7051(7)	598(45)
Se(1B)	4799.7(12)	795.4(7)	6523.0(8)	580(4)
Se(2B)	2654.4(12)	669.7(6)	6666.4(7)	498(4)
Fe(1B)	3204.4(14)	1639.1(9)	5709.9(9)	414(5)
Fe(2B)	3332.5(15)	1886.2(9)	7109.3(9)	436(5)
P(1B)	1352(3)	2543(2)	5512(2)	366(8)
P(2B)	1352(3)	2657(2)	7188(2)	392(8)
O(1B)	3083(10)	622(6)	4419(5)	776(39)
O(2B)	4600(9)	2929(6)	5078(6)	823(41)
O(3B)	4680(10)	3299(6)	6791(6)	780(40)
O(4B)	3919(10)	1580(6)	8689(6)	861(43)
C(1B)	3141(11)	1022(7)	4931(7)	530(41)
C(2B)	4057(11)	2395(8)	5338(7)	575(44)
C(3B)	4115(11)	2756(8)	6912(7)	536(42)
C(4B)	3671(12)	1686(7)	8064(7)	537(42)
C(5B)	886(11)	3238(6)	6287(6)	436(35)
C(6B)	1423(10)	3303(6)	4712(6)	403(34)
C(7B)	1538(11)	4153(6)	4779(6)	515(40)
C(8B)	1739(15)	4655(8)	4160(9)	755(58)
C(9B)	1860(14)	4345(9)	3470(8)	730(56)
C(10B)	1712(14)	3490(9)	3391(7)	698(54)

Table 3 (continued)

Atom	x	y	z	U_{eq}
C(11B)	1490(13)	2991(8)	4023(7)	616(48)
C(12B)	-102(10)	2140(6)	5302(6)	410(34)
C(13B)	-1219(11)	2703(8)	4983(8)	607(46)
C(14B)	-2334(12)	2403(9)	4845(9)	750(56)
C(15B)	-2398(12)	1533(8)	4991(8)	709(54)
C(16B)	-1307(12)	982(7)	5285(8)	622(48)
C(17B)	-176(11)	1278(7)	5412(7)	547(42)
C(18B)	1076(11)	3530(6)	7836(6)	465(37)
C(19B)	-196(12)	3966(7)	7977(7)	606(46)
C(20B)	-378(15)	4628(9)	8477(9)	777(58)
C(21B)	638(16)	4847(8)	8819(8)	755(59)
C(22B)	1885(15)	4424(8)	8676(8)	751(58)
C(23B)	2096(13)	3763(7)	8187(8)	639(48)
C(24B)	38(10)	2075(7)	7405(6)	471(37)
C(25B)	-1150(12)	2221(9)	7063(7)	638(49)
C(26B)	-2134(14)	1769(9)	7244(8)	691(55)
C(27B)	-1892(16)	1139(10)	7829(10)	876(71)
C(28B)	-751(16)	990(9)	8170(9)	779(61)
C(29B)	240(14)	1443(8)	7996(8)	656(49)

Table 4

Atomic coordinates ($\times 10^4$) and equivalent isotropic thermal parameters ($\mathring{A}^2 \times 10^4$) defined as one-third of the trace of the orthogonalized U_{ij} tensor, for the non-hydrogen atoms of the complex **5**

Atom	x	y	z	U_{eq}
Se(1)	416.8(8)	1450.2(5)	119.3(3)	402(2)
Se(2)	992.0(8)	3040.4(5)	1189.9(3)	419(2)
Fe(1)	1946.9(10)	2808.3(6)	125.8(5)	346(3)
Fe(2)	-749.8(11)	1795.1(7)	1111.7(5)	442(3)
Fe(3)	2072.5(11)	1483.3(7)	1107.9(5)	436(3)
P	575.9(17)	3700.2(11)	-603.7(8)	311(5)
O(1)	3711(7)	1933(5)	-879(3)	854(27)
O(2)	4078(6)	4295(5)	524(3)	760(24)
O(3)	4928(7)	2253(6)	1573(4)	1033(33)
O(4)	1541(7)	583(4)	2406(3)	791(25)
O(5)	3276(10)	-263(6)	560(4)	1189(38)
O(6)	-1561(7)	2154(5)	2505(3)	748(24)
O(7)	-2125(10)	-104(5)	1076(3)	1127(36)
O(8)	-3183(7)	2838(6)	431(3)	972(31)
C(1)	3007(8)	2277(5)	-490(4)	507(26)
C(2)	3251(7)	3707(5)	363(3)	458(24)
C(3)	3788(9)	1958(7)	1381(4)	671(33)
C(4)	1667(9)	951(6)	1892(4)	570(29)
C(5)	2786(12)	417(7)	776(5)	797(39)
C(6)	-1230(8)	2010(5)	1971(4)	522(27)
C(7)	-1578(11)	629(7)	1085(4)	729(36)
C(8)	-2240(9)	2425(7)	699(4)	615(31)
C(9)	-480(6)	4636(4)	-200(3)	337(19)
C(10)	-782(7)	3011(5)	-1124(3)	401(21)
C(11)	-2249(8)	3124(6)	-1101(3)	569(28)
C(12)	-3232(10)	2557(8)	-1498(5)	816(40)
C(13)	-2701(13)	1891(8)	-1938(5)	880(42)
C(14)	-1260(12)	1786(7)	-1976(4)	773(38)
C(15)	-279(10)	2342(6)	-1571(4)	636(30)
C(16)	1416(7)	4382(4)	-1265(3)	365(20)
C(17)	560(8)	4690(6)	-1835(4)	543(27)
C(18)	1159(10)	5222(6)	-2344(4)	641(32)
C(19)	2592(11)	5472(6)	-2267(4)	649(33)
C(20)	3468(10)	5157(7)	-1707(4)	753(37)
C(21)	2858(9)	4620(6)	-1207(3)	573(29)

Table 5
Atomic coordinates ($\times 10^4$) and isotropic thermal parameters ($\text{Å}^2 \times 10^4$), for the non-hydrogen atoms of the complex 7

Atom	x	y	z	U
Se(1)	6041.5(13)	2261.0(16)	6547.8(7)	373(8) [a]
Se(2)	7846.6(13)	356.3(16)	6713.9(7)	372(8) [a]
Fe(1)	7168(2)	1536(2)	7362(1)	332(11) [a]
Fe(3)	6674(2)	1275(2)	5906(1)	375(11) [a]
Fe(2)	6035(2)	54(2)	6626(1)	384(11) [a]
P(1)	8299(3)	3061(4)	7482(2)	324(19) [a]
P(2)	7888(3)	2844(4)	5806(2)	369(20) [a]
O(1)	8364(9)	-100(12)	8202(5)	665(41)
O(2)	5952(9)	2539(11)	8113(5)	562(39)
O(3)	5590(8)	-682(11)	7691(5)	561(38)
O(4)	6272(9)	-2456(13)	6229(5)	780(45)
O(5)	3911(11)	140(12)	6032(6)	986(51)
O(6)	5149(10)	1752(12)	5010(6)	805(46)
O(7)	7451(10)	-665(13)	5213(6)	847(48)
C(1)	7886(13)	585(16)	7881(7)	437(52)
C(2)	6434(13)	2149(16)	7805(7)	476(53)
C(3)	5791(13)	-331(17)	7300(8)	568(59)
C(4)	6210(13)	-1471(17)	6400(7)	578(62)
C(5)	4787(16)	99(17)	6270(8)	703(65)
C(6)	5860(15)	1616(16)	5372(8)	583(60)
C(7)	7260(14)	120(17)	5503(8)	630(62)
C(8)	8954(11)	3382(13)	6906(6)	289(45)
C(9)	8227(11)	3959(15)	6394(6)	373(46)
C(10)	7892(11)	4607(13)	7638(6)	280(43)
C(11)	6881(12)	5006(16)	7459(7)	465(54)
C(12)	6579(13)	6186(16)	7587(7)	523(54)
C(13)	7301(13)	6975(16)	7895(7)	546(56)
C(14)	6305(12)	6612(15)	6047(6)	402(51)
C(15)	8600(11)	5432(14)	7922(6)	333(47)
C(16)	9337(11)	2767(14)	8078(6)	302(43)
C(17)	9111(13)	2835(15)	8594(7)	464(53)
C(18)	9897(13)	2558(16)	9064(8)	583(59)
C(19)	10848(14)	2254(16)	8981(8)	613(59)
C(20)	11065(14)	2188(16)	8483(8)	652(62)
C(21)	10323(12)	2447(15)	8018(7)	468(53)
C(22)	9150(11)	2569(14)	5666(6)	263(44)
C(23)	9755(13)	3576(15)	5585(6)	477(53)
C(24)	10784(13)	3471(16)	5507(7)	544(58)
C(25)	11179(13)	2275(17)	5510(7)	515(55)
C(26)	10574(12)	1234(17)	5585(6)	479(52)
C(27)	9592(13)	1406(16)	5662(6)	502(56)
C(28)	7303(12)	3698(17)	5253(7)	456(51)
C(29)	6828(14)	4992(19)	5338(9)	810(71)
C(30)	6340(17)	5760(24)	4882(10)	1206(94)
C(31)	6331(16)	5371(20)	4371(9)	937(77)
C(32)	6801(14)	4350(19)	4268(8)	764(68)
C(33)	7321(14)	3564(18)	4706(8)	686(66)

[a] U_{eq} defined as one-third of the trace of the orthogonalized $\mathbf{U}_{ij}$ tensor.

fact, the IR spectra in the carbonyl region of the double clusters 5, 6 (dppe) and 9 (dppfc), in CH_2Cl_2 solution, are practically identical; furthermore, 5 and 6 give the same fragmentation pattern in their NICl mass spectra. Compound 6 should be a positional isomer of 5, one or two P atoms probably being coordinated in equatorial positions.

The IR spectra of the disubstituted, isostructural,

bridged derivatives 3 (dppm), 7 (dppe) and 8 (dppfc) exhibit slightly different patterns. As discussed below, this should be related to significant differences in the structural parameters of the Fe_3Se_2 core induced by the different bites of the three ligands. Compounds 3 and 7 exhibit complex ^{31}P NMR spectra, suggesting fluxional behaviour in solution. In particular, the spectrum of 3 at room temperature (Fig. 1) shows a singlet (δ 77.7) and two doublets at higher fields (δ 53.0 and 42.6, $J(P,P)$ 58 Hz). Correspondingly, the ^{1}H NMR spectrum shows two triplets at 4.08 and 3.22 ppm (area ratio 1:1 in chloroform and 3:2 in toluene), which gives coalescence in toluene at 364 K.

These data suggest fluxional behaviour for 3 in solution due to the migration of an iron–iron bond from a side of the open triangle to the basal plane of the square pyramid linking the two iron atoms bound to the bidentate ligand. In this way the two phosphorus atoms become unequivalent and give the observed doublets in the ^{31}P NMR spectrum. The singlet at lower fields is obviously attributed to the other isomer, the only isolable in the solid state. This isomerism is probably induced by the dppm ligand, whose steric demand causes the basal iron atoms to approach, promoting linking between them.

In the case of the corresponding dppe derivative 7, the same dynamic behaviour appears to take place. However, the ^{31}P NMR spectrum is more complex, showing a single peak at 75.9 ppm due to the isomer isolated in the solid state (two equivalent P atoms) and three other peaks. These peaks are attributable to a single species (the less symmetrical isomer), the area of one of them (δ 68.3) being the sum of those of the other two; probably this isomer undergoes another fluxional behaviour, involving exchange between the equatorial and axial positions, favoured by the flexibility of the dppe ligand.

Finally, the dynamic behaviour described above, apparently due to a metal–metal bond migration, is not observed in the case of the ligand dppfc (single ^{31}P peak at 73.7 ppm). The only isomer present in solution is the same as isolated in the solid state, and this is in agreement with the larger bite of this ligand, which actually favours a larger distance between the two basal iron atoms.

3.2. Description of the crystal structures

The molecular structures of $[Fe_3(\mu_3\text{-}Se)_2(CO)_7(dppm)]$ 3, $[Fe_2(\mu\text{-}Se_2)(CO)_4(dppm)]$ 4, $[\{Fe_3(\mu_3\text{-}Se)_2(CO)_8\}_2(dppe)]$ 5, $[Fe_3(\mu_3\text{-}Se)_2(CO)_7(dppe)]$ 7 and $[Fe_3(\mu_3\text{-}Se)_2(CO)_7(dppfc)]$ 8 are shown in Figs. 2–6 respectively, together with the atomic labelling systems. The most important bond distances and angles are given in Table 7, Table 8, Table 9, Table 10, and Table 11.
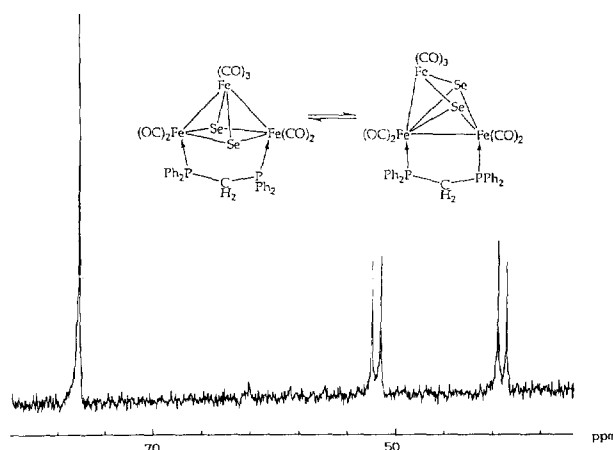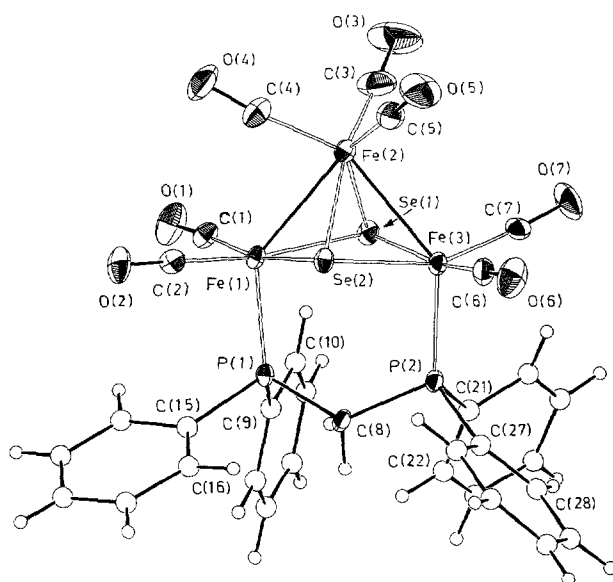
Table 6
Atomic coordinates ($\times 10^4$) and isotropic thermal parameters ($\mathring{A}^2 \times 10^4$) for the non-hydrogen atoms of the complex **8**

Atom	x	y	z	U
Se(1)	2937.1(5)	675.7(7)	600.4(4)	396(3) [a]
Se(2)	3297.9(5)	1892.9(7)	1819.5(4)	376(3) [a]
Fe(1)	2010.7(7)	1255.7(10)	1114.0(5)	400(5) [a]
Fe(2)	3309.1(7)	-22.7(10)	1629.0(5)	411(5) [a]
Fe(3)	4209.1(6)	1429.7(9)	1280.1(5)	339(4) [a]
Fe(4)	2557.5(6)	4335.1(9)	146.2(5)	349(4) [a]
P(1)	1226.1(11)	2591.1(17)	554.1(9)	335(8) [a]
P(2)	4438.2(12)	2965.0(17)	847.1(9)	322(8) [a]
O(1)	1383(5)	1517(9)	2143(3)	1218(48) [a]
O(2)	823(5)	-427(6)	470(4)	1103(42) [a]
O(3)	2475(5)	-2032(6)	1064(4)	1117(47) [a]
O(4)	4965(4)	-1033(6)	2047(3)	830(35) [a]
O(5)	2894(6)	-353(8)	2741(4)	1304(53) [a]
O(6)	5149(5)	50(6)	713(3)	809(36) [a]
O(7)	5648(4)	1765(6)	2413(3)	786(32) [a]
C(1)	1616(5)	1408(9)	1735(5)	688(45) [a]
C(2)	1274(6)	240(8)	716(5)	590(42) [a]
C(3)	2803(6)	-1246(8)	1286(5)	668(49) [a]
C(4)	4348(6)	-564(8)	1873(4)	571(41) [a]
C(5)	3079(6)	-214(9)	2319(5)	730(48) [a]
C(6)	4783(5)	612(7)	929(4)	477(37) [a]
C(7)	5089(5)	1651(8)	1967(4)	514(39) [a]
C(8)	1689(4)	3900(6)	537(3)	351(31) [a]
C(9)	2428(5)	4335(6)	995(4)	326(31) [a]
C(10)	2556(5)	5399(7)	836(4)	438(37) [a]
C(11)	1895(6)	5651(7)	277(5)	513(42) [a]
C(12)	1369(5)	4744(7)	86(4)	444(36) [a]
C(13)	635(4)	2337(6)	-271(3)	333(18)
C(14)	926(5)	1620(7)	-597(4)	493(23)
C(15)	497(6)	1460(8)	-1233(5)	734(30)
C(16)	-241(6)	2050(8)	-1517(5)	731(30)
C(17)	-541(6)	2757(7)	-1193(4)	564(25)
C(18)	-113(5)	2918(8)	-566(4)	466(22)
C(19)	386(5)	2928(6)	860(3)	403(20)
C(20)	370(5)	3889(7)	1149(4)	514(24)
C(21)	-251(6)	4073(8)	1426(4)	659(28)
C(22)	-813(6)	3264(8)	1395(4)	734(30)
C(23)	-819(7)	2350(9)	1106(4)	764(30)
C(24)	-224(6)	2120(8)	812(4)	612(26)
C(25)	3630(4)	3559(6)	185(3)	330(30) [a]
C(26)	3624(5)	4641(7)	-36(4)	446(38) [a]
C(27)	2914(6)	4752(8)	-585(4)	499(41) [a]
C(28)	2491(6)	3758(8)	-710(4)	491(39) [a]
C(29)	2925(5)	3026(7)	-247(3)	370(32) [a]
C(30)	4824(4)	4152(6)	1355(3)	343(19)
C(31)	5339(5)	4916(7)	1213(4)	534(24)
C(32)	5594(6)	5845(8)	1576(4)	678(29)
C(33)	5344(6)	5985(8)	2079(5)	704(29)
C(34)	4851(6)	5238(8)	2233(4)	614(26)
C(35)	4596(5)	4302(7)	1873(4)	450(21)
C(36)	5294(5)	2729(6)	544(3)	415(20)
C(37)	5148(6)	2611(7)	-74(4)	536(24)
C(38)	5829(6)	2324(8)	-273(5)	735(30)
C(39)	6588(7)	2185(8)	147(5)	734(30)
C(40)	6744(7)	2300(8)	758(5)	730(30)
C(41)	6101(5)	2577(7)	970(4)	580(25)
C(42A)	2205(15)	766(20)	7742(11)	1047(72)
C(42B)	3092(21)	912(29)	8038(18)	1746(121)
Cl(1A)	2883(7)	-92(10)	7541(6)	1464(37)
Cl(2A)	2598(8)	512(12)	8684(6)	1694(40)
Cl(3A)	2643(7)	2121(8)	7820(5)	1354(32)

Table 6 (continued)

Atom	x	y	z	U
Cl(1B)	2734(16)	-435(20)	7832(12)	2145(102)
Cl(2B)	2958(25)	1086(34)	8606(21)	3056(200)
Cl(3B)	2798(10)	2058(14)	7527(8)	1159(59)
Cl(1C)	2693(11)	305(15)	7218(9)	1231(63)
Cl(2C)	2367(16)	50(23)	8331(15)	2073(110)
Cl(3C)	2451(20)	1897(28)	8117(16)	2879(153)

[a] U_{eq} defined as one-third of the trace of the orthogonalized $\mathbf{U}_{ij}$ tensor.

Fig. 1. ^{31}P NMR spectrum of **3** at room temperature with the scheme of the proposed dynamic behaviour.

Fig. 2. Perspective view of the structure of the complex [Fe$_3$(μ_3-Se)$_2$(CO)$_7$(dppm)] **3** with the atomic labelling scheme. The thermal ellipsoids are drawn at the 30% probability level.

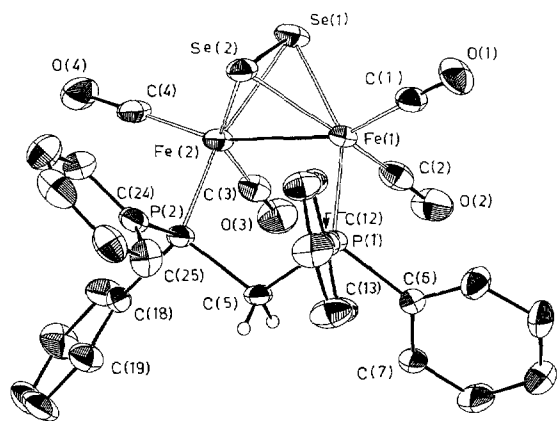Fig. 3. Perspective view of the structure of the complex [Fe$_2$(μ-Se$_2$)(CO)$_4$(dppm)] **4** (molecule A) with the atomic labelling scheme. The thermal ellipsoids are drawn at the 30% probability level.

Clusters **3**, **5**, **7** and **8** have the well-known bicapped open triangular structure Fe$_3$Se$_2$, and should be regarded as *nido*-clusters with seven skeletal electron pairs. The structure of these compounds could also be described as a square pyramid with two iron and two selenium atoms alternating in the basal plane and the third iron atom (Fe$_{ap}$) at the apex of the pyramid. The four atoms which define the base of the pyramid present significant distortions from planarity, being the two Se atoms directed slightly towards the apical Fe atom, and the dihedral angles along the Se–Se line range from 163.07(7)° for **3** to 175.17(6)° for **8**, while for the unsubstituted cluster **1** a value of 166° was found [15].
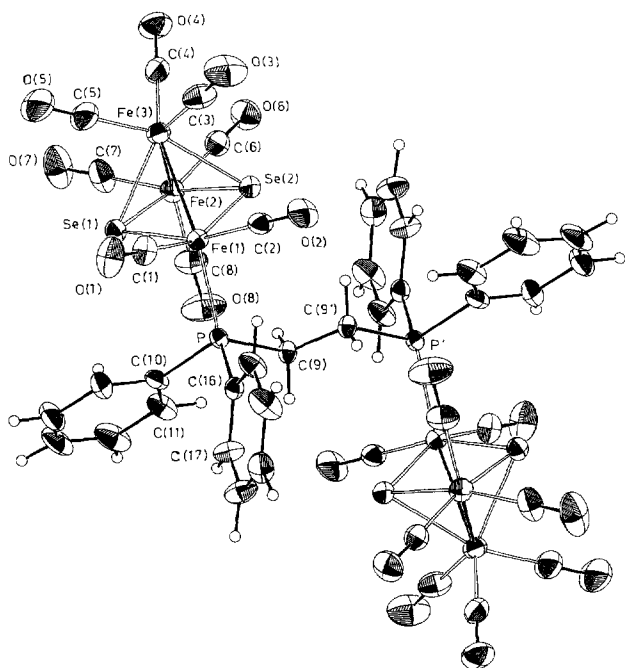

Fig. 4. Perspective view of the structure of the complex [{Fe$_3$(μ_3-Se)$_2$(CO)$_8$}$_2$(dppe)] **5** with the atomic labelling scheme. The thermal ellipsoids are drawn at the 30% probability level.

Fig. 5. Perspective view of the structure of the complex [Fe$_3$(μ_3-Se)$_2$(CO)$_7$(dppe)] **7** with the atomic labelling scheme. The thermal ellipsoids are drawn at the 30% probability level.

The orientation of the apical Fe(CO)$_3$ fragment with respect to the four basal atoms is such that a CO group lies roughly in the plane defined by the three Fe atoms and interacts weakly through the C atom with the nearest basal Fe atom at a distance ranging from 2.71(2) Å for **7** to 2.851(8) Å for **5**. A different orientation was found in **1**, [Fe$_3$(μ_3-Se)$_2$(CO)$_8$(PPh$_3$)] [4] and in [Fe$_3$(μ_3-Se)$_2$(CO)$_7$(PPh$_3$)$_2$] [5], where a CO group lies roughly in the plane defined by the apical Fe atom and the two Se atoms.

The phosphine substitution is regioselective, occurring only on the two basal iron atoms; in [Fe$_3$(μ_3-Se)$_2$(CO)$_8$(PPh$_3$)] and [Fe$_3$(μ_3-Se)$_2$(CO)$_7$(PPh$_3$)$_2$] the

Fig. 6. Perspective view of the structure of the complex [Fe$_3$(μ_3-Se)$_2$(CO)$_7$(dppfc)] **8** with the atomic labelling scheme. The thermal ellipsoids are drawn at the 30% probability level.

Table 7
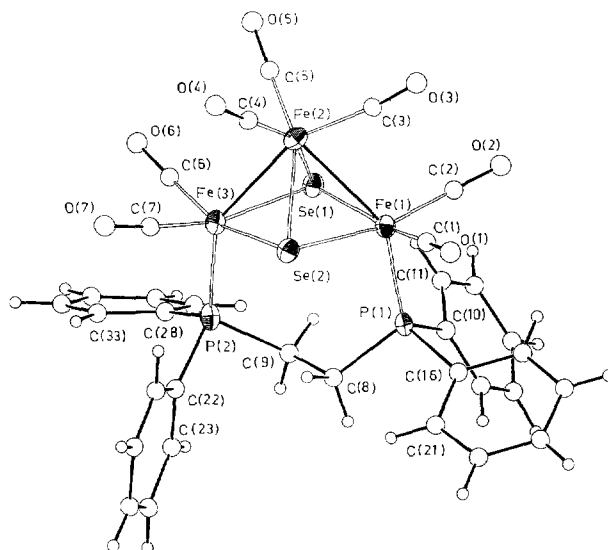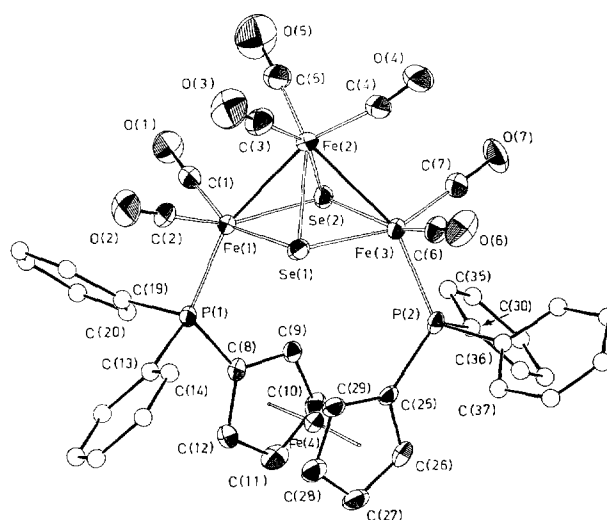Selected bond distances (Å) and angles (°) for complex **3**

Se(1)-Fe(1)	2.361(2)	Se(2)-Fe(1)	2.371(2)
Se(1)-Fe(2)	2.371(2)	Se(2)-Fe(2)	2.380(2)
Se(1)-Fe(3)	2.351(2)	Se(2)-Fe(3)	2.368(2)
Fe(1)-Fe(2)	2.690(2)	Fe(2)-Fe(3)	2.679(2)
Fe(1)-P(1)	2.193(3)	Fe(3)-P(2)	2.224(3)
Fe(2)-Se(1)-Fe(3)	69.1(1)	Fe(1)-Se(1)-Fe(2)	69.3(1)
Fe(1)-Se(1)-Fe(3)	95.5(1)	Fe(1)-Se(2)-Fe(3)	94.8(1)
Fe(2)-Se(2)-Fe(3)	68.7(1)	Fe(1)-Se(2)-Fe(2)	69.0(1)
Se(1)-Fe(1)-Se(2)	83.3(1)	Se(1)-Fe(3)-Se(2)	83.6(1)
Se(2)-Fe(1)-Fe(2)	55.7(1)	Se(2)-Fe(3)-Fe(2)	55.9(1)
Se(1)-Fe(1)-Fe(2)	55.5(1)	Se(1)-Fe(3)-Fe(2)	55.8(1)
Se(2)-Fe(2)-Fe(1)	55.3(1)	Se(2)-Fe(2)-Fe(3)	55.4(1)
Se(1)-Fe(2)-Fe(1)	55.2(1)	Se(1)-Fe(2)-Fe(3)	55.1(1)
Se(1)-Fe(2)-Se(2)	82.9(1)	Fe(1)-Fe(2)-Fe(3)	81.1(1)
Se(2)-Fe(1)-P(1)	94.9(1)	Se(2)-Fe(3)-P(2)	96.5(1)
Se(1)-Fe(1)-P(1)	92.8(1)	Se(1)-Fe(3)-P(2)	90.5(1)
Fe(2)-Fe(1)-P(1)	136.0(1)	Fe(2)-Fe(3)-P(2)	135.6(1)
P(1)-O(8)-P(2)	120.4(5)		

phosphines occupy equatorial positions, while in **3**, **7** and **8**, for steric requirements, they occupy axial positions as well as in **5**, in which the phosphine acts as a bridging ligand.

Despite the different nature and different type of coordination of the phosphine in these clusters, it is not possible to correlate the variations observed in the Fe–Fe and Fe–Se bond distances, while a significant

Table 8
Selected bond distances (Å) and angles (°) for complex **4**

Molecule A		Molecule B	
Se(1)-Se(2)	2.294(2)	Se(1)-Se(2)	2.293(2)
Se(1)-Fe(1)	2.384(2)	Se(1)-Fe(1)	2.381(2)
Se(1)-Fe(2)	2.362(2)	Se(1)-Fe(2)	2.363(2)
Se(2)-Fe(1)	2.388(2)	Se(2)-Fe(1)	2.386(2)
Se(2)-Fe(2)	2.363(2)	Se(2)-Fe(2)	2.362(2)
Fe(1)-Fe(2)	2.579(2)	Fe(1)-Fe(2)	2.577(2)
Fe(1)-P(1)	2.194(3)	Fe(1)-P(1)	2.190(3)
Fe(2)-P(2)	2.185(3)	Fe(2)-P(2)	2.193(3)
Fe(1)-Se(1)-Fe(2)	65.8(1)	Fe(1)-Se(1)-Fe(2)	65.8(1)
Se(2)-Se(1)-Fe(2)	61.0(1)	Se(2)-Se(1)-Fe(2)	60.9(1)
Se(2)-Se(1)-Fe(1)	61.3(1)	Se(2)-Se(1)-Fe(1)	61.4(1)
Se(1)-Se(2)-Fe(2)	60.9(1)	Se(1)-Se(2)-Fe(2)	61.0(1)
Se(1)-Se(2)-Fe(1)	61.2(1)	Se(1)-Se(2)-Fe(1)	61.1(1)
Fe(1)-Se(2)-Fe(2)	65.8(1)	Fe(1)-Se(2)-Fe(2)	65.7(1)
Se(1)-Fe(1)-Se(2)	57.5(1)	Se(1)-Fe(1)-Se(2)	57.5(1)
Se(2)-Fe(1)-P(1)	103.3(1)	Se(2)-Fe(1)-P(1)	102.9(1)
Se(2)-Fe(1)-Fe(2)	56.7(1)	Se(2)-Fe(1)-Fe(2)	56.7(1)
Se(1)-Fe(1)-P(1)	151.8(1)	Se(1)-Fe(1)-P(1)	151.5(1)
Se(1)-Fe(1)-Fe(2)	56.7(1)	Se(1)-Fe(1)-Fe(2)	56.8(1)
Fe(2)-Fe(1)-P(1)	96.1(1)	Fe(2)-Fe(1)-P(1)	95.7(1)
Se(2)-Fe(2)-Fe(1)	57.6(1)	Se(2)-Fe(2)-Fe(1)	57.6(1)
Se(1)-Fe(2)-Fe(1)	57.5(1)	Se(1)-Fe(2)-Fe(1)	57.4(1)
Se(1)-Fe(2)-Se(2)	58.1(1)	Se(1)-Fe(2)-Se(2)	58.0(1)
Fe(1)-Fe(2)-P(2)	95.3(1)	Fe(1)-Fe(2)-P(2)	95.6(1)
Se(2)-Fe(2)-P(2)	94.7(1)	Se(2)-Fe(2)-P(2)	95.1(1)
Se(1)-Fe(2)-P(2)	148.2(1)	Se(1)-Fe(2)-P(2)	148.6(1)
P(1)-O(5)-P(2)	110.9(5)	P(1)-C(5)-P(2)	111.2(5)

Table 9
Selected bond distances (Å) and angles (°) for complex **5**

Se(1)-Fe(1)	2.357(1)	Se(1)-Fe(2)	2.363(1)
Se(1)-Fe(3)	2.371(1)	Se(2)-Fe(3)	2.394(1)
Se(2)-Fe(1)	2.367(1)	Se(2)-Fe(2)	2.359(1)
Fe(1)-Fe(3)	2.666(2)	Fe(2)-Fe(3)	2.645(2)
Fe(1)-P	2.211(2)		
Fe(2)-Se(1)-Fe(3)	67.9(1)	Fe(2)-Se(2)-Fe(3)	67.6(1)
Fe(1)-Se(1)-Fe(3)	68.7(1)	Fe(1)-Se(2)-Fe(3)	68.1(1)
Fe(1)-Se(1)-Fe(2)	98.6(1)	Fe(1)-Se(2)-Fe(2)	98.4(1)
Se(1)-Fe(1)-Se(2)	81.0(1)	Se(1)-Fe(2)-Se(2)	81.1(1)
Se(2)-Fe(1)-Fe(3)	56.4(1)	Se(1)-Fe(1)-Fe(3)	55.9(1)
Se(2)-Fe(2)-Fe(3)	56.8(1)	Se(1)-Fe(2)-Fe(3)	56.2(1)
Fe(1)-Fe(3)-Fe(2)	84.7(1)	Se(1)-Fe(3)-Se(2)	80.2(1)
Se(2)-Fe(3)-Fe(2)	55.6(1)	Se(1)-Fe(3)-Fe(2)	55.9(1)
Se(2)-Fe(3)-Fe(1)	55.5(1)	Se(1)-Fe(3)-Fe(1)	55.4(1)
Se(2)-Fe(1)-P	105.3(1)	Se(1)-Fe(1)-P	97.8(1)
Fe(3)-Fe(1)-P	147.7(1)		

Table 10
Selected bond distances (Å) and angles (°) for complex **7**

Se(1)-Fe(1)	2.381(3)	Se(1)-Fe(3)	2.376(3)
Se(1)-Fe(2)	2.390(3)	Se(2)-Fe(2)	2.405(3)
Se(2)-Fe(1)	2.374(3)	Se(2)-Fe(3)	2.364(3)
Fe(1)-Fe(2)	2.648(3)	Fe(3)-Fe(2)	2.651(4)
Fe(1)-P(1)	2.210(5)	Fe(3)-P(2)	2.214(5)
Fe(3)-Se(1)-Fe(2)	67.6(1)	Fe(1)-Se(1)-Fe(2)	67.4(1)
Fe(1)-Se(1)-Fe(3)	96.9(1)	Fe(1)-Se(2)-Fe(3)	97.4(1)
Fe(3)-Se(2)-Fe(2)	67.5(1)	Fe(1)-Se(2)-Fe(2)	67.3(1)
Se(1)-Fe(1)-Se(2)	82.3(1)	Se(1)-Fe(3)-Se(2)	82.6(1)
Se(2)-Fe(1)-Fe(2)	56.9(1)	Se(2)-Fe(3)-Fe(2)	57.0(1)
Se(1)-Fe(1)-Fe(2)	56.4(1)	Se(1)-Fe(3)-Fe(2)	56.5(1)
Fe(1)-Fe(2)-Fe(3)	84.4(1)	Se(1)-Fe(2)-Se(2)	81.4(1)
Se(2)-Fe(2)-Fe(3)	55.5(1)	Se(2)-Fe(2)-Fe(1)	55.8(1)
Se(1)-Fe(2)-Fe(3)	56.0(1)	Se(1)-Fe(2)-Fe(1)	56.1(1)
Se(1)-Fe(1)-P(1)	99.3(2)	Se(1)-Fe(3)-P(2)	96.7(2)
Se(2)-Fe(1)-P(1)	98.2(2)	Se(2)-Fe(3)-P(2)	100.1(2)
Fe(2)-Fe(1)-P(1)	144.9(2)	Fe(2)-Fe(3)-P(2)	144.2(2)

Table 11
Selected bond distances (Å) and angles (°) for complex **8**

Se(1)-Fe(1)	2.382(2)	Se(1)-Fe(3)	2.378(1)
Se(1)-Fe(2)	2.395(2)	Se(2)-Fe(2)	2.405(2)
Se(2)-Fe(1)	2.365(1)	Se(2)-Fe(3)	2.366(2)
Fe(1)-Fe(2)	2.637(2)	Fe(2)-Fe(3)	2.654(2)
Fe(1)-P(1)	2.229(2)	Fe(3)-P(2)	2.237(3)
Fe(4)-M(1)	1.655(10)	Fe(4)-M(2)	1.653(10)
Fe(2)-Se(1)-Fe(3)	67.6(1)	Fe(1)-Se(2)-Fe(2)	67.1(1)
Fe(1)-Se(1)-Fe(3)	99.2(1)	Fe(1)-Se(2)-Fe(3)	100.1(1)
Fe(1)-Se(1)-Fe(2)	67.0(1)	Fe(2)-Se(2)-Fe(3)	67.6(1)
Se(1)-Fe(1)-Se(2)	80.2(1)	Se(1)-Fe(3)-Se(2)	80.3(1)
Se(2)-Fe(1)-Fe(2)	57.2(1)	Se(2)-Fe(3)-Fe(2)	56.9(1)
Se(1)-Fe(1)-Fe(2)	56.7(1)	Se(1)-Fe(3)-Fe(2)	56.5(1)
Se(2)-Fe(2)-Fe(1)	55.7(1)	Se(2)-Fe(2)-Fe(3)	55.5(1)
Se(1)-Fe(2)-Fe(1)	56.3(1)	Se(1)-Fe(2)-Fe(3)	55.9(1)
Se(1)-Fe(2)-Se(2)	79.1(1)	Fe(1)-Fe(2)-Fe(3)	86.5(1)
Se(2)-Fe(1)-P(1)	112.3(1)	Se(2)-Fe(3)-P(2)	106.0(1)
Se(1)-Fe(1)-P(1)	107.4(1)	Se(1)-Fe(3)-P(2)	107.2(1)
Fe(2)-Fe(1)-P(1)	160.5(1)	Fe(2)-Fe(3)-P(2)	156.1(1)
M(1)-Fe(4)-M(2)	176.0(4)		

M(1) and M(2) are the centroids of the cyclopentadienyl rings.

Table 12

Comparison between structural parameters in the cluster cores of the clusters $[Fe_3(\mu_3\text{-Se})_2(CO)_7(LL)]$, $[LL = dppm$ (3), dppe (7), dppfc (8), $(PPh_3)_2$ (10)] and $[\{Fe_3(\mu_3\text{-Se})_2(CO)_8\}_2(dppe)]$ (5)

	3 dppm	7 dppe	8 dppfc	10 $(PPh_3)_2$	5 $1/2$ dppe
Fe...Fe (Å)	3.489(2)	3.560(4)	3.626(2)	3.527(2)	3.578(2)
Se...Se (Å)	3.144(2)	3.130(3)	3.057(1)	3.101(1)	3.069(1)
Fe-Se-Fe(°) [a]	95.18(6)	97.1(1)	99.66(6)	96.45(3)	98.58(4)
Se-Fe-Se (°) [a]	83.43(5)	82.4(1)	80.21(5)	81.96(3)	81.06(4)
Fe-Fe$_{ap}$-Fe (°)	81.05(6)	84.4(1)	86.54(6)	81.01(3)	84.73(4)
Se-Fe$_{ap}$-Se(°)	82.87(6)	81.4(1)	79.14(5)	81.88(3)	80.20(4)
Fe$_{ap}$-Fe-P (°) [a]	135.8(1)	144.5(2)	158.3(1)	112.50(1) [b]	147.7(1)

[a] Average of two data.
[b] PPh_3 in equatorial positions.

correlation was found by analyzing bond angles and non-bonding distances.

Table 12 reports the comparison of the structural parameters in the Fe_3Se_2 core for clusters 3, 7, 8, in which the dppm, dppe and dppfc ligands bridge the two basal positions, for the cluster $[Fe_3(\mu_3\text{-Se})_2(CO)_7(PPh_3)_2]$ 10 [4] and for 5, where the dppe bridges two cluster units.

By passing from dppm to dppe and dppfc, we can observe a progressive variation of the structural parameters, owing to the steric demand of the diphosphines linking the basal iron atoms. In particular, the Fe · · · Fe non-bonding distance increases while the Se · · · Se one decreases with parallel deformation of the angles at the base and on the top of the pyramid. If we assume that the cluster cores of the PPh_3-disubstituted compound 10 and of 5 are unstrained, then we deduce that the Fe_3Se_2 core in 7, whose structural parameters are well comparable with those of 5 and 10, is the less strained among the basal bridged compounds. The dppm ligand forces the open triangular cluster to bring the basal iron atoms close, whereas dppfc forces them to move them away. As expected, the Fe_{ap}–Fe–P angles undergo a significant increase on passing from dppm to dppfc.

In 3 the two P atoms of the dppm molecule are essentially coplanar with the three Fe atoms [maximum deviation from the mean plane passing through the five atoms 0.080(2) Å for P(2)] and the methylene carbon atom C(8) is out of this plane by 0.592(9) Å; the P(1)–C(8)–P(2) angle value is 120.4(5)°, significantly larger than the theoretical one, and indicative of the strain of the dppm molecule. Also, in the case of 7 the P atoms of dppe are coplanar with the three Fe atoms [maximum deviation from the mean plane passing through the five atoms 0.067(5) Å for P(2)], but the angles at both methylene carbon atoms C(8) and C(9) do not present significant distortion from the theoretical value [113(1)° for both]. In 8 the planarity of the P_2Fe_3 system is preserved [maximum deviation from the mean plane passing through the five atoms 0.071(2) Å for

P(1)], and also the Fe atom of the ferrocene group is coplanar [0.098(1) Å].

In 5 the dppe molecule bridges two Fe_3Se_2 cores through the P atoms that occupy axial positions. The complex has an imposed C_i symmetry with the inversion centre lying on the midpoint of the CH_2CH_2 bond.

In 4 two independent, but very similar, $[Fe_2(\mu\text{-}Se_2)(CO)_4(dppm)]$ complexes are present, where the Fe–Fe and Se–Se bond distances in the Fe_2Se_2 tetrahedral core are 2.579(2) and 2.294(2) Å (molecule A) and 2.577(2) and 2.293(2) Å (molecule B), whereas the Fe–Se bond distances range between 2.362(2) and 2.388(2) Å. The dppm ligand bridges the Fe atoms and the two P atoms lie in the Fe(1)Se(1)Fe(2) plane. The Fe–Fe bond distances in 4 are very similar to those found in the unsubstituted complex $Fe_2Se_2(CO)_6$ [16] (2.575(1) Å), moreover the P–C–P bond angles (110.9(5)° for A and 111.2(5)° for B) do not reveal any strain for the dppm molecules. This is in agreement with the fluxional behaviour found for 3, where the dppm molecule can span bonded or non-bonded Fe atoms.

References

[1] G. Hogarth, N.J. Taylor, A.J. Carty and A. Meyer, J. Chem. Soc., Chem. Commun., (1988) 834.

[2] S.M. Stuczynski, Y.-U. Kwon and M.L. Steigerwald, J. Organomet. Chem., 449 (1993) 167.

[3] W. Imhof and G. Huttner, J. Organomet. Chem., 448 (1993) 247.

[4] P. Baistrocchi, D. Cauzzi, M. Lanfranchi, G. Predieri, A. Tiripicchio and M. Tiripicchio Camellini, Inorg. Chim. Acta, 235 (1995) 173.

[5] P. Baistrocchi, M. Carezi, D. Cauzzi, C. Graiff, M. Lanfranchi, P. Manini, G. Predieri and A. Tiripicchio, Inorg. Chim. Acta, 252 (1996) 367.

[6] D. Cauzzi, C. Graiff, M. Lanfranchi, G. Predieri and A. Tiripicchio, J. Chem. Soc., Dalton Trans., (1995) 2321.

[7] A.M. Bond, R. Colton and P. Panagiotidou, Organometallics, 7 (1988) 1767.

[8] E.W. Ainscough, H.A. Bergen, A.M. Brodie and K.A. Brown, *J. Chem. Soc., Dalton Trans.*, (1976) 1649.

[9] N. Walker and D. Stuart, *Acta Crystallogr., A39* (1983) 158; F. Ugozzoli, *Comput. Chem., 11* (1987) 109.

[10] G.M. Sheldrick, SHELXS-86, *Program for the Solution of Crystal Structures*, Universität Göttingen, Germany, 1986.

[11] G.M. Sheldrick, SHELX-76, *Program for Crystal Structure Determination*, University of Cambridge, UK, 1976.

[12] *International Tables for X-Ray Crystallography*, Vol. IV, Kynoch Press, Birmingham, UK, 1974, pp. 99–102, 149.

[13] W. Hieber and J. Gruber, *Z. Anorg. Allg. Chem., 296* (1958) 91; G. Cetini, P.L. Stanghellini, R. Rossetti and O. Gambino, *J. Organomet. Chem., 15* (1968) 373.

[14] P.A. Wegner, L.F. Evans and J. Haddock, *Inorg. Chem., 14* (1975) 192; R.L. Keiter, A.L. Rheingold, J.J. Hamerski and C.K. Castle, *Organometallics, 2* (1983) 1635; S. Cartwright, J.A. Clucas, R.H. Dawson, D.F. Foster, M.M. Harding and A. Smith, *J. Organomet. Chem., 302* (1986) 403.

[15] L.F. Dahl and P.W. Sutton, *Inorg. Chem., 2* (1963) 1067.

[16] C.F. Campana, F.Y.-K. Lo and L.F. Dahl, *Inorg. Chem., 18* (1979) 3060.